

By acceptance of this article, the publisher or recipient acknowledges the U.S. Government's right to retain a nonexclusive, royalty-free license in and to any copyright covering the article.

MASTER

DEMONSTRATION OF DIRECT ENERGY RECOVERY OF FULL ENERGY IONS
AT 40keV ON A PLT/ISX BEAM SYSTEM*

W. L. Stirling, G. C. Barber, W. K. Dagenhart, R. R. Feezell,
W. L. Gardner, H. H. Haselton, J. Kim, M. Menon, N. S. Ponte,
C. C. Tsai, and J. H. Whealton

Oak Ridge National Laboratory, Oak Ridge, Tennessee, 37830

* Research sponsored by the Office of Fusion Energy, U.S. Department of Energy, under contract W-7405-eng-26 with the Union Carbide Corporation.

DISCLAIMER

This book was prepared as an account of work sponsored by an agency of the United States Government. Neither the United States Government nor any agency thereof, nor any of their employees, makes any warranty, express or implied, or assumes any legal liability or responsibility for the accuracy, completeness, or usefulness of any information, apparatus, product, or process disclosed, or represents that its use would not infringe privately owned rights. Reference herein to any specific commercial product, process, or service by trade name, trademark, manufacturer, or otherwise, does not necessarily constitute or imply its endorsement, recommendation, or favoring by the United States Government or any agency thereof. The views and opinions of authors expressed herein do not necessarily state or reflect those of the United States Government or any agency thereof.

DISTRIBUTION OF THIS DOCUMENT IS UNLIMITED



Summary

The injection of neutral hydrogen or deuterium particles continues to be the most promising means of heating magnetically confined fusion plasmas to ignition temperatures. Neutral beam injection systems that employ positive ion sources presently operate at energies of about 40-50 keV/nucleon at 60 A [Princeton Large Torus (PLT)] or 100 A [Princeton Divertor Experiment or the Oak Ridge National Laboratory (ORNL) Impurities Study Experiment (ISX)] with about 50-60% conversion efficiency. However, the desire for multisecond beams in the 80-keV/nucleon energy range at 10 MW/module has emphasized the need for technological advances in several areas. At such beam energies, as much as 75% of the initial beam energy is retained in the unneutralized ion components. As a result, two questions immediately come to mind: (1) how can one dispose of this energy; or better still, how can one efficiently recover this energy? The conventional way of treating such a problem is to deflect the ions out of the neutral beam and onto water-cooled plates or beam dumps. This method has worked satisfactorily for 40-keV/nucleon beams in excess of 1.5 MW and ~0.5 s. However, the power per unit area to be disposed of in the high power, multi-second beams mentioned above is beyond present-day technology. We have proposed and demonstrated a unique solution to this problem which not only removes the need for beam dumps but also returns from 50-80% of the energy contained in the full energy ion component directly and dynamically to the high voltage supply. In fact, the energy in the residual ion component is not expended. The tests were made on a PLT/ISX type beam line at 40 keV/nucleon of about 800 kW and 0.1 s.

A number of investigators^{1,2} have been at work for many years attempting to develop an efficient, stable means of recovering the energy in the ~~unneutralized~~ unneutralized component of a neutral beam system. The need for such a system is illustrated in Fig. 1 in which the efficiency of a neutral beam system with and without energy recovery is plotted. Without recovery, 75-80% of the system energy is wasted in the 80-100 keV neutron range. With recovery, assuming a 90% atomic species in the beam, 40-60% of the energy is lost. Besides the induced energy loss, the energy which is lost is removed at a much lower power density than that achieved in a conventional beam system.

As an example of a conventional neutral beam line, Fig. 2 illustrates the 40-kV, 60-A beam line used in recent neutral beam heating experiments in the PLT device and in ISX-B. The ion source is maintained at a high positive potential of typically 40 kV, and the beam of positive ions is accelerated to its full energy in the usual accel-decel manner. The accel potential extracts the ions from the plasma source and gives them their final energy. The decel potential

prevents secondary electrons generated in the gas cell from being back accelerated through the exit grid into the plasma grid.

The beam of positive ions extracted from the ion source is thus accelerated to ground potential and remains at ground potential through the gas cell neutralizer and the magnet region of the beam line. In the gas cell, some of the positive ions from the ion source are converted to neutral particles and are used in the normal sense, i.e., for injection into a fusion plasma. The magnet, located along the beam line a short distance beyond the gas cell, has pole pieces tilted at 45° for the purpose of deflecting the unneutralized full, one-half, and one-third energy ions to their respective water-cooled ion dumps. The only role of the magnetic field is to separate the unneutralized ions that come out of the gas cell at high energy waste that energy in striking the ion beam dump.

We have developed a means of both recovering a large fraction of the ion energy that is otherwise wasted and alleviating the problem of high power density beam disposal.³ This energy recovery system employs a combination of crossed magnetic and electric fields at the gas or neutralizer cell exit. Figure 3 shows a comparison of the potential distribution along a conventional beam line with that along the energy recovery beam system. In the latter, the ion source is maintained slightly above ground potential by a voltage V_{boost} in the range of 0-5 kV. As usual, an accel voltage V_{accel} and a decel voltage V_{decel} are employed. The gas cell is held at the same potential as the exit grid, i.e., at $-V$, which is shown as -40 kV typical. A guard ring or electron dump that functions as an electron collector is fastened around the end opening of the gas cell by means of small electrical insulators (see Fig. 4). The guard ring is maintained slightly positive by a conducting collar that floats at a potential $V_{\text{collector}}$, which is maintained slightly positive (several thousand volts) with respect to the gas cell potential of $-V$. The magnet and all of the walls of the vacuum chamber are at ground potential. The atomic ions proceeding from the gas cell exit return their energy to the high voltage supply, losing only the small amount by which the ion source is biased above ground. In this arrangement, all ground surfaces serve as a collector. The one-half and one-third energy ions cannot escape the gas cell and thus terminate on the gas cell itself. The high atomic yield (85% for the Oak Ridge duoPIGatron⁴) permits the maximum obtainable recovery efficiency for present-day sources.

Of course, even higher proton yields are desirable.

The retarding field seen by the emerging full energy ions also tries to accelerate electrons from the gas cell (as illustrated in Fig. 4). The role of the transverse magnetic field is to impede the electron flow. Coupling of the magnetic field with the axial electric field causes the electrons to $E \times B$ drift into the concentric electron collector or dump (which is slightly positive with respect to the gas cell), thereby losing a negligible amount of energy (patent pending). The recovery efficiency quoted above is achieved with electron losses included. The proton recovery efficiency is 70%.

The critical component of this recovery system is the interface between the gas cell exit, the transverse magnetic field, and the axial electric field. The two interface geometries studied are shown in Fig. 5. In both versions, V_{ec} is the electron collector bias supply.

The two interfaces differ in the way in which one-half and one-third energy ions are terminated. In the loose coupled scheme, these ions turn around and strike an interior wall of the gas cell extension. In this manner, no secondary electrons emitted can cause a power drain since they are produced inside the gas cell. In the close coupled scheme, the close proximity of the ground plane causes the fractional energy ions to be reflected back into the gas cell with the result, again, of no electron power drain.

Both interfaces have been tested in the manner indicated by Fig. 6. The current difference, $I_B - I_A$ or boost supply current minus accel supply current, yields the ion recovery current (including electron loss to ground). In our experiments to date, we have had a small recovery current due to limitations imposed by our boost supply. Thus, the error has been large as we have obtained a small difference between two large numbers. The net current recovery efficiency has been obtained by dividing the ion recovery current minus the electron current by the ion current available for recovery. The latter is calculated from calorimetric power measurements knowing the beam system transmission efficiency, the ion source fractions, and the equilibrium cell neutral fraction for each species as a function of energy. All of these factors are well known for the PLT/ISX beam system. Figure 7 is a summary of the results.

Figure 8 shows a variation of the recovery efficiency as a function of the magnetic field strength for three different beam conditions using the loose coupled interface. As the beam density (current) becomes higher, the magnetic field required to achieve a given efficiency also becomes higher.

Figure 9 shows the variation of the recovery efficiency for the close coupled interface efficiency for the close coupled with the boost voltage for two magnetic field current settings. Also shown is the full energy positive ion recovery efficiency at each magnetic field condition. To first order, the electron loss is independent of a boost voltage above 500 V. As can be seen, the efficiency increases with magnetic field. Earlier results, not shown, yielded an efficiency greater than 60% for a magnetic field current of 500 A.

Figure 10 shows the electron loss to the ground surface, located immediately above the collector ring. Electrons that miss the collector for any reason should have a high probability of striking this particular ground surface. A B^{-1} variation is also shown since the electron drift velocity is inversely proportional to B. At a magnet current of between 200 A and 300 A, the electron loss is greater than expected but varies as B^{-1} at currents above 350 A. The loss at currents below 200 A has not been investigated.

A critical factor in the success of this energy recovery method will be the loss of electrons with beam current density and the effect of the magnetic field at higher current densities. Experiments to date have been up to a beam density of 14 ma/cm^2 at the gas cell exit, which is within a factor of 3 to 4 of that required for a reactor relevant beam system. Thus far, electron losses are easily controlled, and computational tools are being developed to aid in the design of a more efficient geometry for the gas cell interface.

EFFICIENCY OF NEUTRAL BEAM INJECTION SYSTEM
WITH AND WITHOUT ENERGY RECOVERY

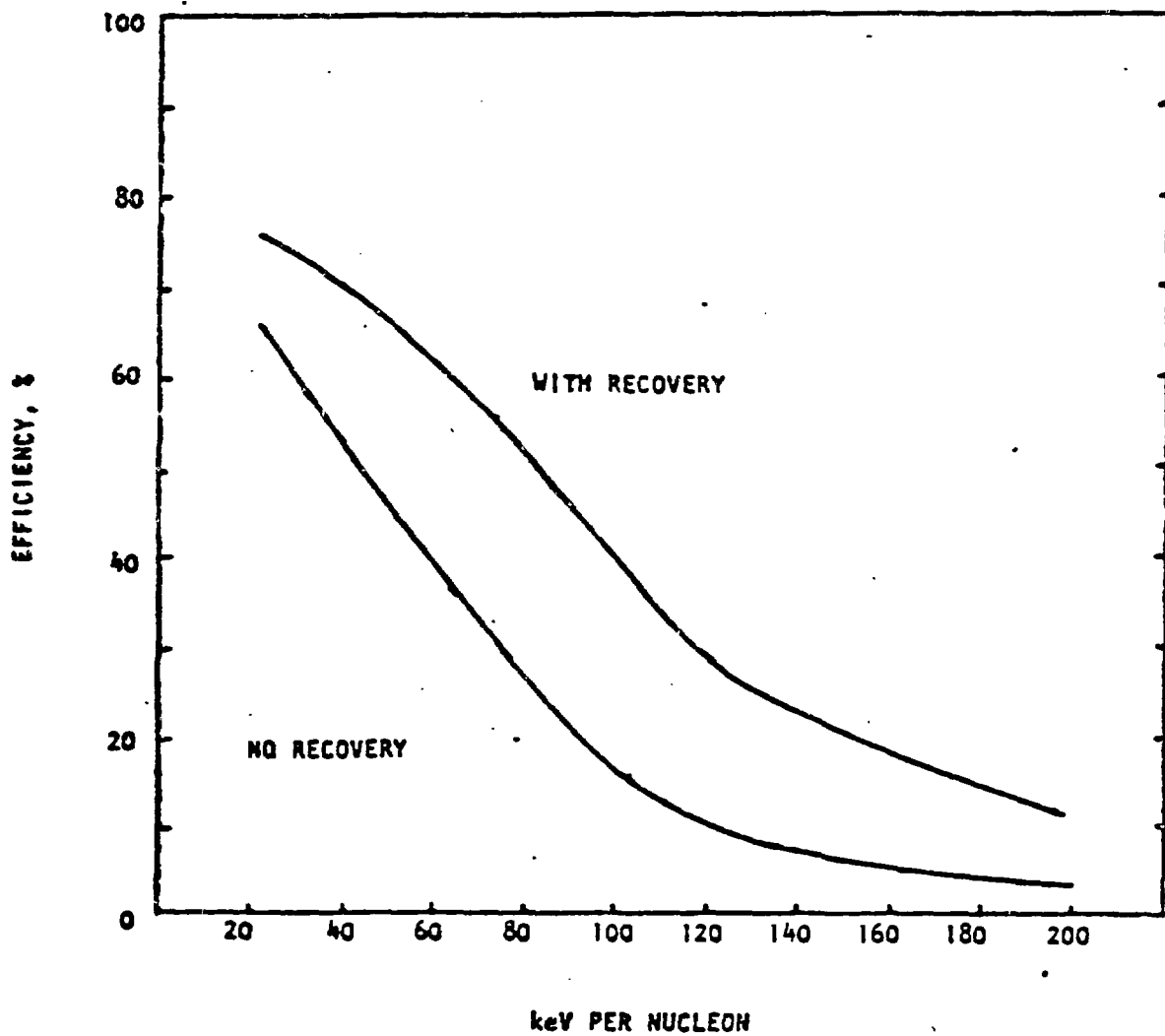


Fig 1

PARTICLE DISPOSAL IN A CONVENTIONAL BEAM LINE

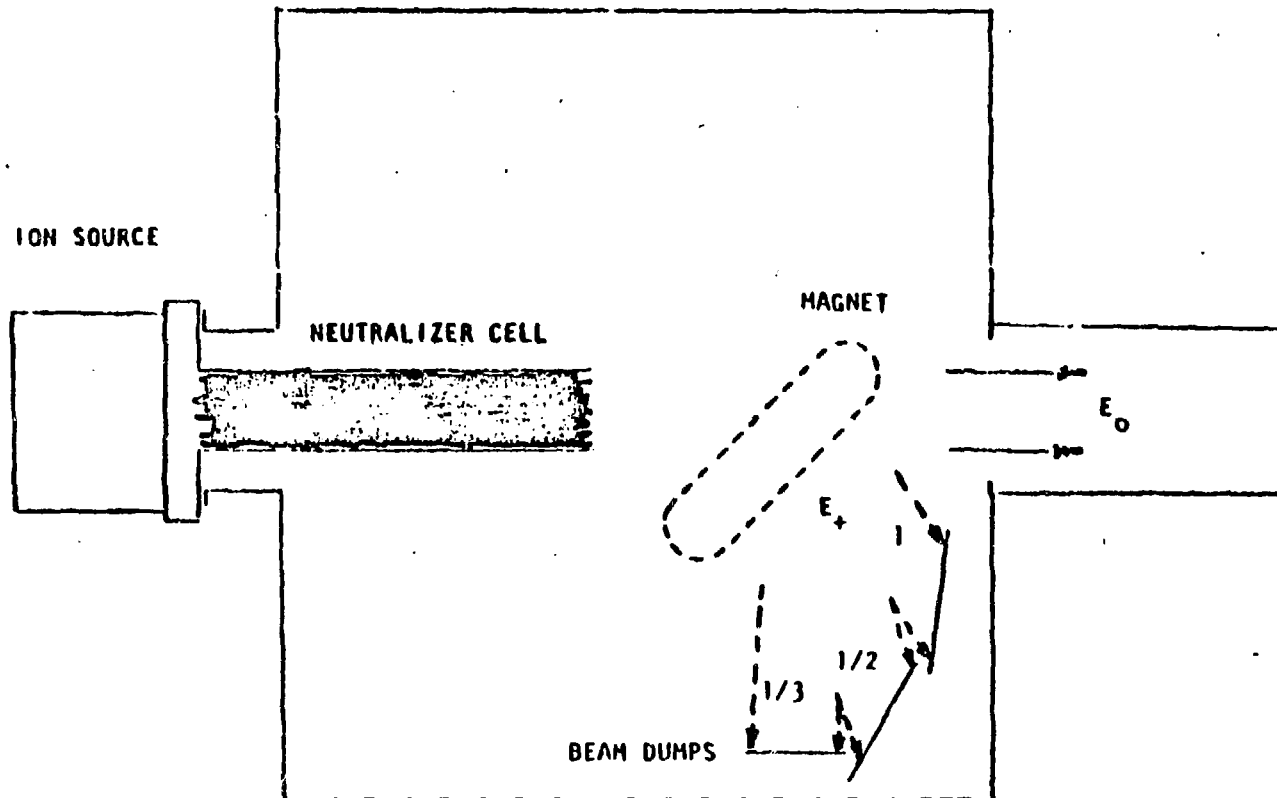


Fig 2

POTENTIAL DISTRIBUTION FOR CONVENTIONAL
AND ENERGY RECOVERY SYSTEMS

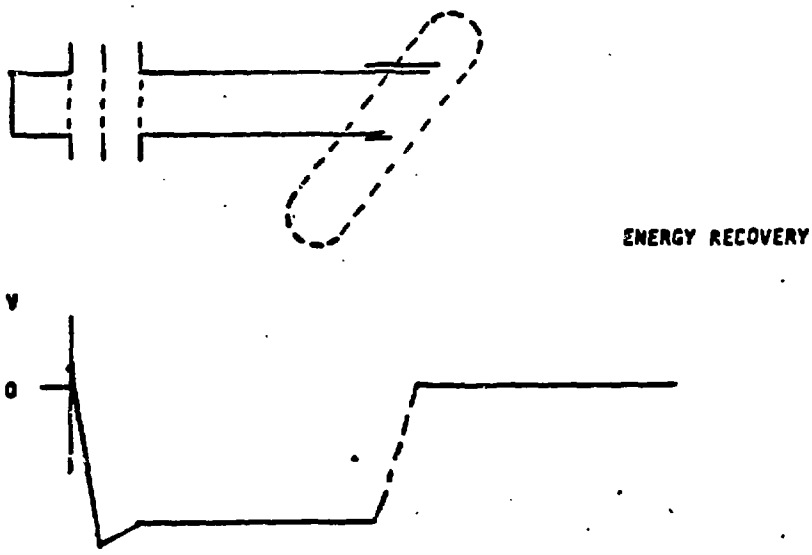
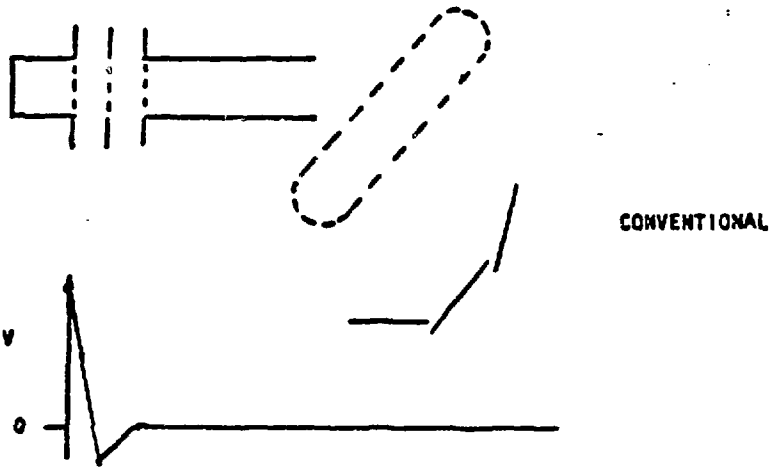
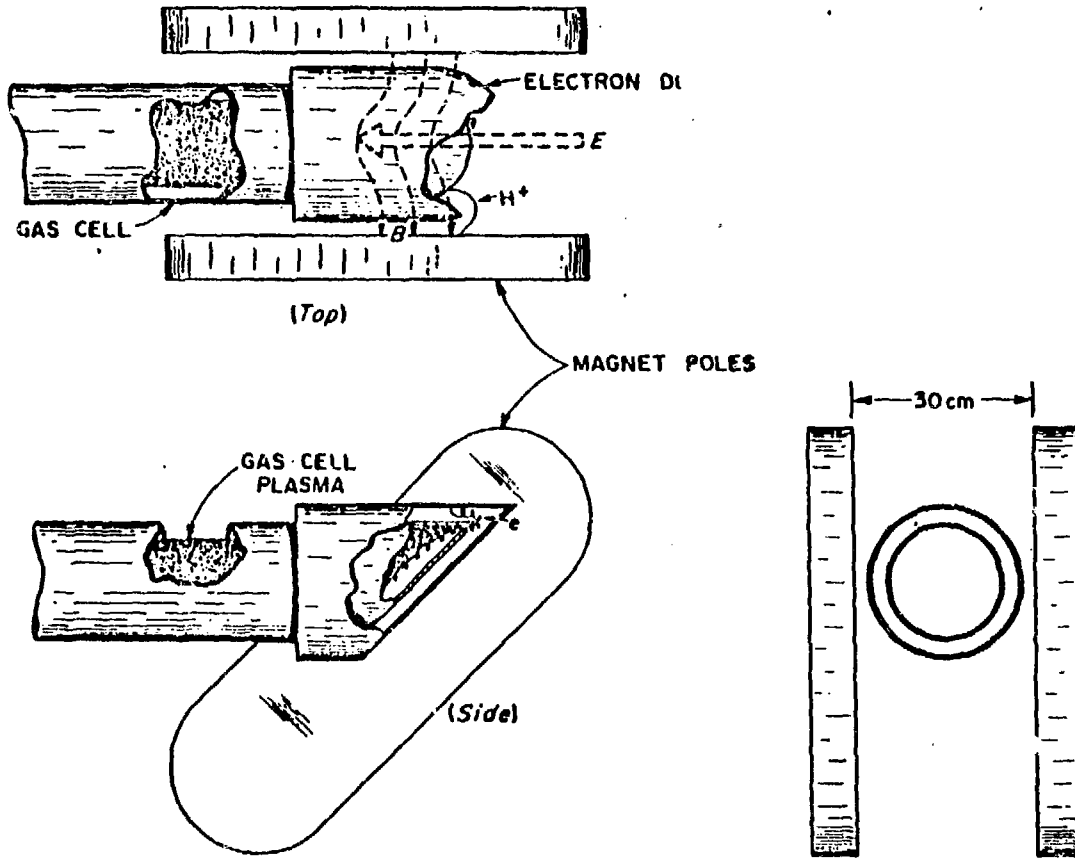


Fig 3



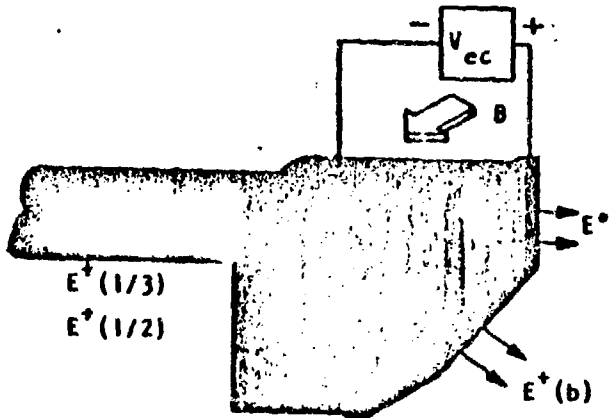
Electron Blocking by Crossed Magnetic Field

Fig 4

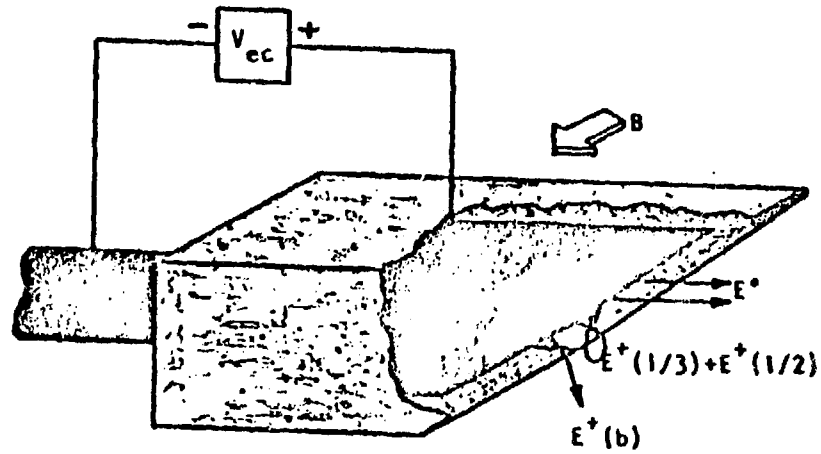
ADVANCED ENERGY RECOVERY SYSTEMS
HAVE BEEN OPERATED

80-3165

— GAS CELL ELECTRON COLLECTOR —
— GAS CELL EXIT GROUND SHIELD —



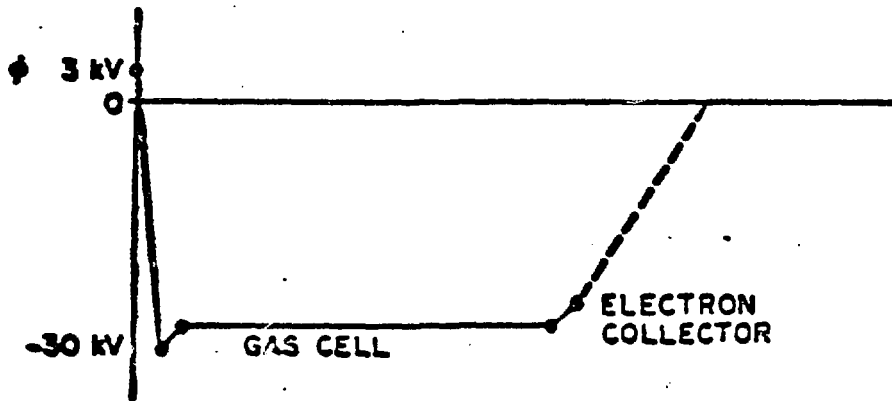
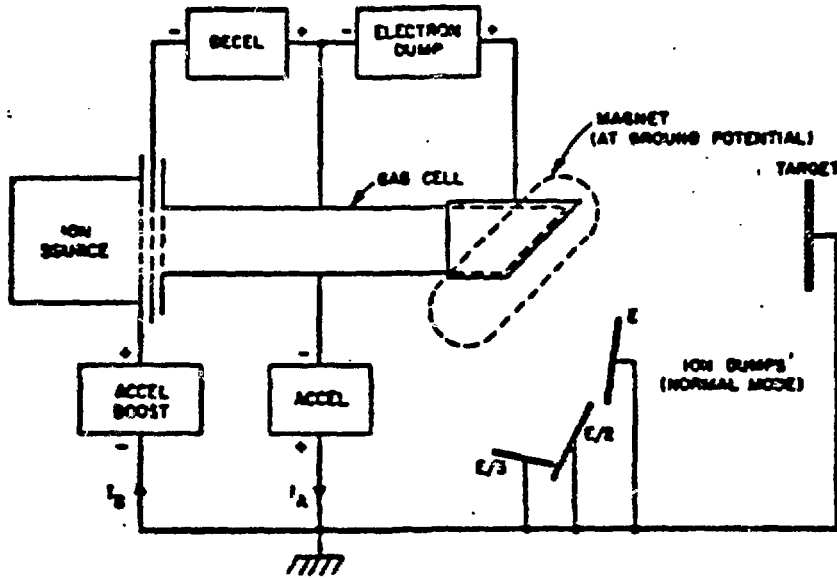
LOOSE COUPLED



CLOSE COUPLED

Fig 5

ELECTRICAL SCHEMATIC



$$I_B = I_0 + I_R + I(1) + I(1/2) + I(1/3)$$

$$I_A = I_0 + I(1) + I(1/2) + I(1/3) + I_0$$

$$I_B - I_A = I_R - I_0$$

Fig 6

WO#

VU#

80-480

RECOVERY EFFICIENCY IS DETERMINED FROM CURRENT
MEASUREMENTS AND BACKED BY POWER MEASUREMENTS

● EFFICIENCY DEFINITION

$$\eta = \frac{\text{RECOVERED ION CURRENT} - \text{ELECTRON LEAKAGE CURRENT}}{\text{AVAILABLE ION CURRENT}}$$

● EFFICIENCY MEASUREMENTS -- 40 keV, 18 A HYDROGEN BEAM

$$\eta_{LC} = 80\% \pm 20\%$$

$$\eta_{CC} = \overset{50}{\cancel{60}}\% \pm 15\%$$

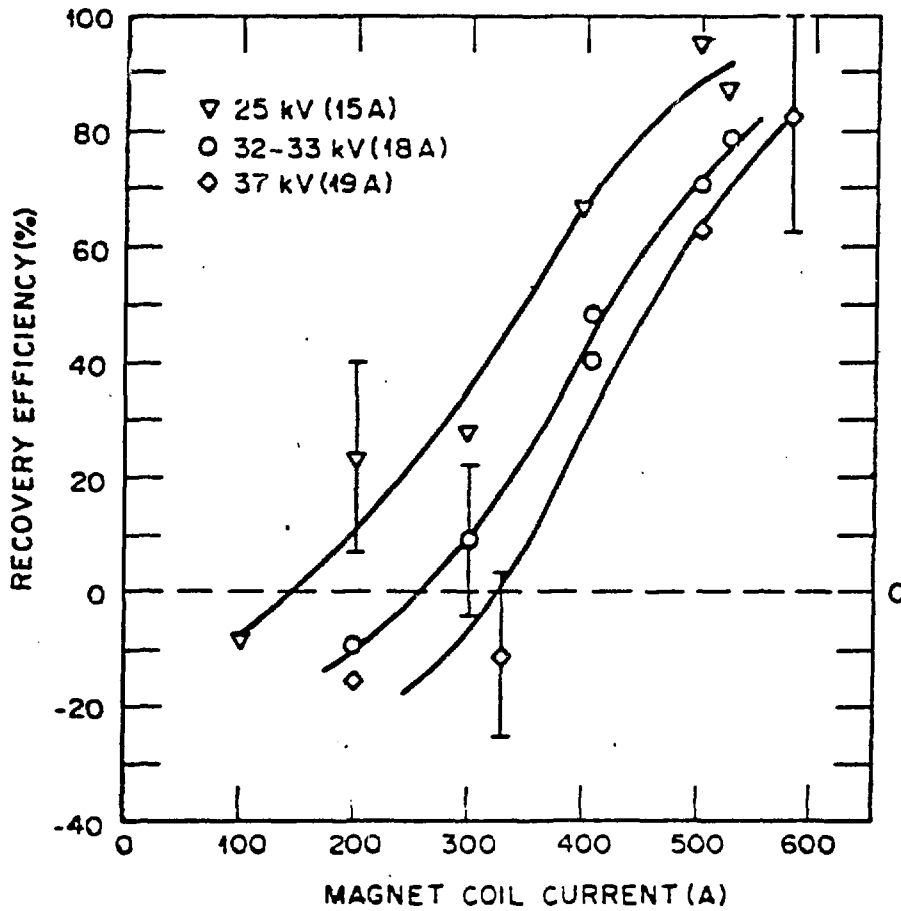
● EFFICIENCY IS INDEPENDENT OF PRESSURE OR PULSE LENGTH

● EFFICIENCY WAS DETERMINED ON A PLT/ISX TYPE BEAM SYSTEM

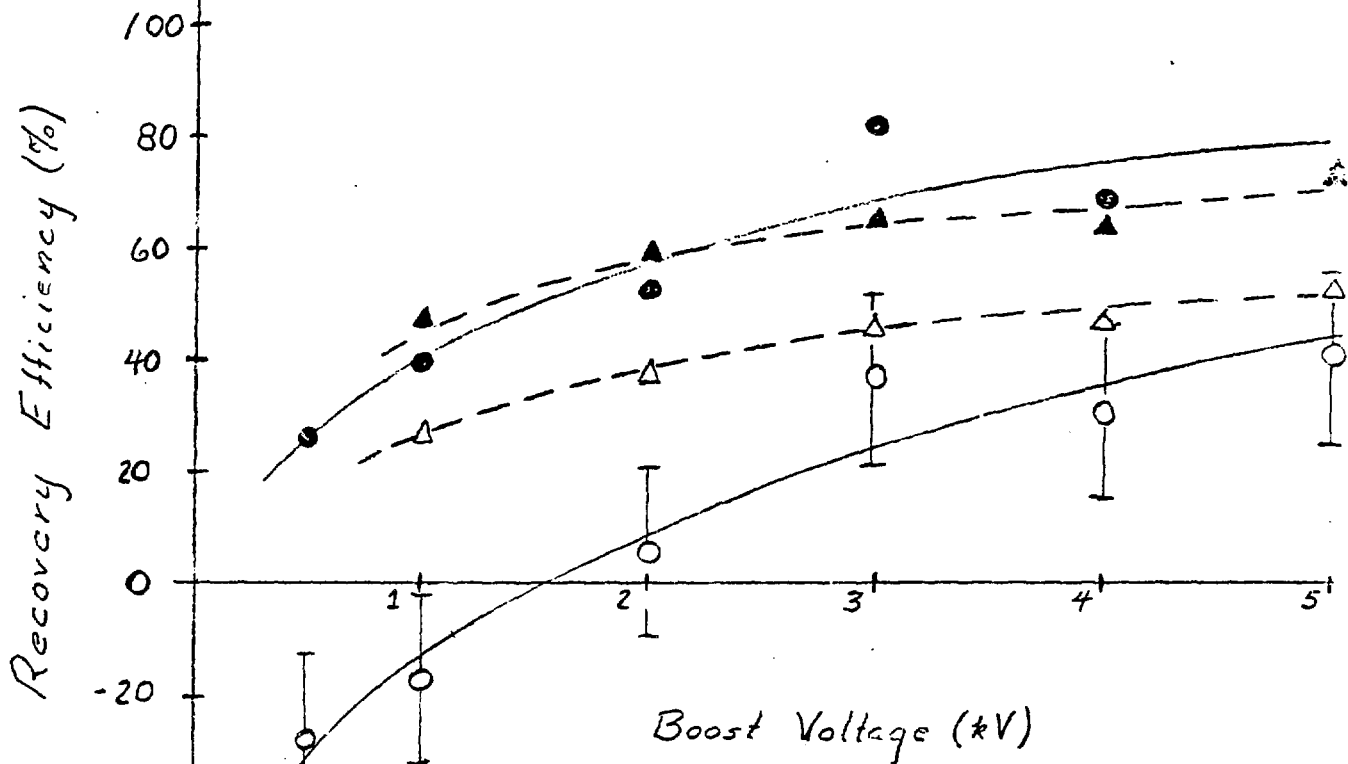
Fig 7

8
F
=

ORNL-DWG 79-2566R FED



Recovery Efficiency as a Function of Boost Voltage
Close Coupled System



$I_M = 250 A$

- Net recovery efficiency
- $H^*(E)$ recovery efficiency

$I_M = 350 A$

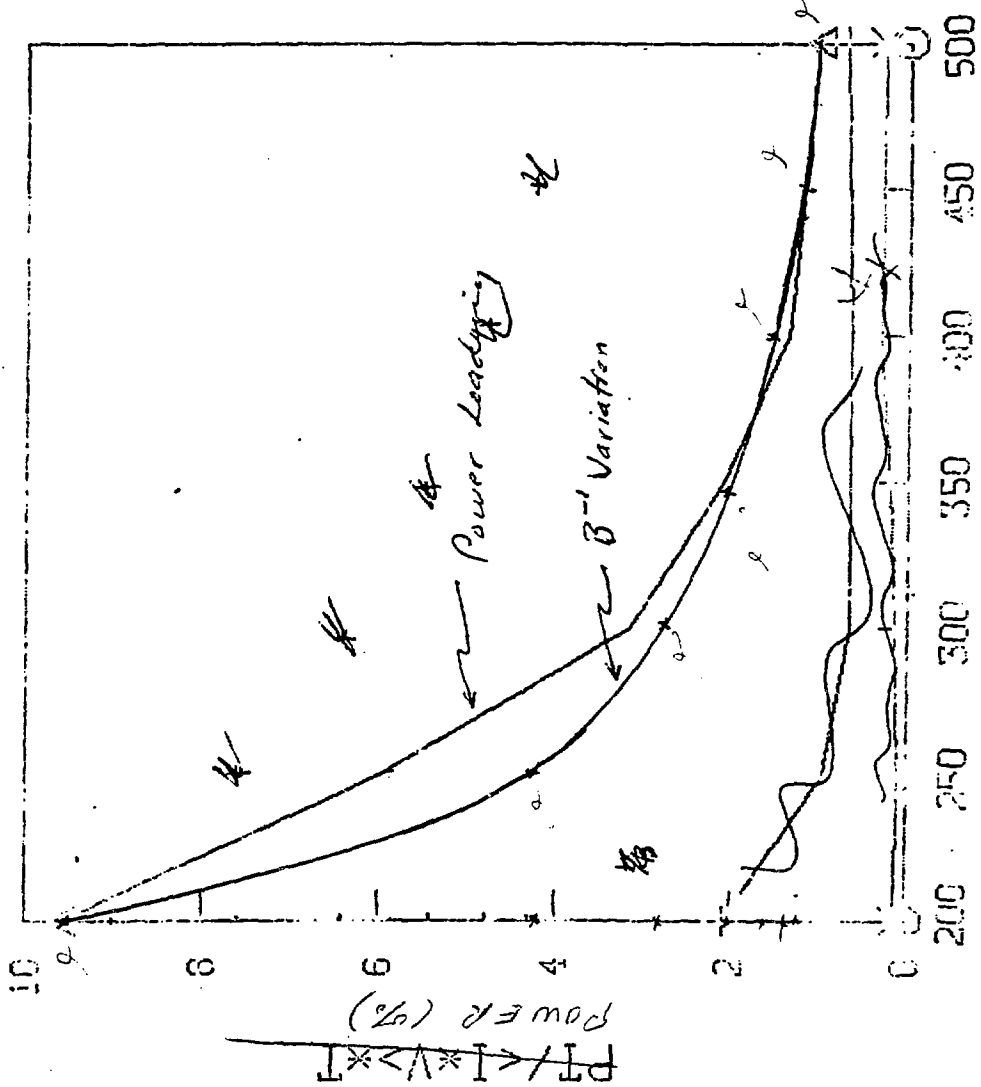
- △ Net recovery efficiency
- ▲ $H^*(E)$ recovery efficiency

ORDER NO: 15-AUG-89 TIME: 20:53
UNIT NO: 12-015-80 TIME: 21:23:06
ID NUMBER: 5

no more odd little

ON TOR GRABNO ELECTRODE

PERCENTAGE POWER LOADING VS BLOCKING CURRENT DENSITY
FOR 10.500 GAUSS. THE CURVE SHOWS A SMOOTH SLOPE. THE
DENSITY IS APPROXIMATELY 1000 A/CM².



CHANN - LRSFL
 13 ELEC RECTP
 16 GRDELCT TP
 5 GRDELCT FR
 25 GRDELCT B

Fig 10
needs drawing:
micrograph
4 1/2" glossy

BLOCKING MAGNET AMPS

References

1. W. L. Barr, R. W. Moir, and G. W. Hamilton, Test Results on a High Power, 100 keV Beam Directed Converter, UCLR-84432, June 3, 1980.
2. M. Fumelli and Ph. Raimbault, "A Scheme for the Energy Recovery of the Charged Beam Fraction in Neutral Injectors," paper presented at the 9th Symposium on Fusion Technology, Garmisch-Partenkirchen, 1976.
3. W. L. Stirling, J. Kim, H. H. Haselton, G. C. Barber, R. C. Davis, W. K. Dagenhart, W. L. Gardner, N. S. Ponte, C. C. Tsai, J. H. Whealton, and R. E. Wright, *Appl. Phys. Lett.* 35, 104-106 (1976).
4. J. Kim, W. L. Stirling, M. Menon, W. K. Dagenhart, G. C. Barber, R. C. Davis, H. H. Haselton, D. E. Schechter, and C. C. Tsai, *J. Appl. Phys.* 51, 1984-93 (1980).

FIGURE CAPTIONS

- Fig. 1. Efficiency of neutral beam injection system with and without energy recovery.
- Fig. 2. Particle disposal in a conventional beam line.
- Fig. 3. Potential distribution for conventional and energy recovery systems.
- Fig. 4. Electron blocking by crossed magnetic field.
- Fig. 5. Interface configurations for the energy recovery system.
- Fig. 6. Electrical schematic for testing of the interface.
- Fig. 7. Recovery efficiency determined from current measurement and backed by power measurements.
- Fig. 8. Recovery efficiency as a function of the magnetic field strength for three beam conditions.
- Fig. 9. Recovery efficiency as a function of boost voltage in a close coupled system.
- Fig. 10. Percentage power loading on top ground electrode vs blocking magnetic field.